JOURNAL OF SOLID STATE CHEMISTRY **140,** 272–277 (1998)
ARTICLE NO. SC987886

$Ba_2(VO_2)(PO_4)(HPO_4)\cdot H_2O$, a New Barium Vanadium(V) Phosphate Hydrate Containing Trigonal Bipyramidal VO_5 Groups

Zsolt Bircsak and William T. A. Harrison[1]

Department of Chemistry, University of Western Australia, Nedlands, WA 6907, Australia

Received November 4, 1997; in revised form April 22, 1998; accepted May 8, 1998

The hydrothermal synthesis, single crystal structure, and some physical properties of $Ba_2(VO_2)(PO_4)(HPO_4)\cdot H_2O$, a new barium vanadium(V) phosphate hydrate, are reported. This phase is built up from one-dimensional chains of unusual VO_5 trigonal bipyramids and $(H)PO_4$ tetrahedra, fused together via V–O–P linkages. These anionic chains propagate along the polar [010] direction. 11-Coordinate barium cations and water molecules occupy the interchain regions and link the chains together. Structural data for this phase and other known barium vanadium phosphates are briefly compared. Crystal data: $Ba_2(VO_2)(PO_4)(HPO_4)\cdot H_2O$, $M_r = 566.57$, monoclinic, space group $P2_1$ (No. 4), $a = 5.0772(5)$ Å, $b = 8.724(2)$ Å, $c = 10.806(1)$ Å, $\beta = 90.795(8)^\circ$, $V = 478.6(1)$ Å^3, $Z = 2$, $R = 2.65\%$, $R_w = 2.89\%$ [147 parameters, 1893 observed reflections with $I > 3\sigma(I)$].

INTRODUCTION

A number of barium vanadium phosphates (BaVPOs) have now been prepared and structurally characterized on the basis of single crystal diffraction data (1–14). As is typical of vanadium compounds, the V cations in these BaVPO phases show flexibility in both oxidation state [V^{III}, V^{IV}, or V^{V}] and coordination preference, leading to wide structural diversity in these materials (*vide infra*). The first mixed-valence [V^{IV} and V^{V}] BaVPOs have been described very recently (13, 14).

In this paper we report the hydrothermal synthesis and single crystal structural characterization of $Ba_2(VO_2)(PO_4)(HPO_4)\cdot H_2O$, a new colorless, noncentrosymmetric barium vanadium(V) phosphate hydrate which contains unusual VO_5 trigonal bipyramids as a component part of one-dimensional $[VO_2(PO_4)(HPO_4)]^{4-}$ anionic chains. The structures of known BaVPO phases are briefly compared.

[1] To whom correspondence should be addressed.

EXPERIMENTAL

Synthesis and initial characterization. $Ba_2(VO_2)(PO_4)(HPO_4)\cdot H_2O$ was prepared from a mixture of $BaCO_3$ (2.19 g), 85% H_3PO_4 (6.40 g), V_2O_5 (0.25 g), and 10 mL deionized water (starting molar ratio of Ba : V : P = 4 : 1 : 20). These components were sealed in a 23-ml capacity Teflon-lined hydrothermal bomb and heated to 120°C for 17 h. After slow cooling, the bomb was opened, and the solid contents recovered by vacuum filtration, resulting in a mixture of at least three types of visually distinct crystals—very pale yellowish blocks of $BaHPO_4$ (15), small transparent crystals of NH_4VO_3 (16), and intergrown transparent plate-like crystals of the title compound. Visual estimation of the yield of $Ba_2(VO_2)(PO_4)(HPO_4)\cdot H_2O$ in this mixture was in the 5–10% range. We have not succeeded in preparing $Ba_2(VO_2)(PO_4)(HPO_4)\cdot H_2O$ in higher yield. Hydrothermal reactions starting from stoichiometric amounts of Ba-, V-, and P-containing precursors led to insignificant amounts of the title compound.

X-ray powder diffraction data [Siemens D5000 automated diffractometer, Cu$K\alpha$ radiation, $\lambda = 1.5418$ Å, $T = 25(2)^\circ$C] were recorded for a well-ground powder sample of $Ba_2(VO_2)(PO_4)(HPO_4)\cdot H_2O$ (hand-separated crystals from the as-synthesized mixture). The use of software "stripping" and peak-fitting routine established peak positions relative to the Cu$K\alpha_1$ ($\lambda = 1.54056$ Å) wavelength. The data were indexed by comparison with a LAZY-PULVERIX (17) simulation of the single crystal structure of $Ba_2(VO_2)(PO_4)(HPO_4)\cdot H_2O$, and least-squares refinement was carried out with the program ERACEL (18) to result in monoclinic cell parameters of $a = 5.066(3)$ Å, $b = 8.725(2)$ Å, $c = 10.801(4)$ Å, and $\beta = 90.80(3)^\circ$ ($V = 477.4$ Å^3). Powder data for $Ba_2(VO_2)(PO_4)(HPO_4)\cdot H_2O$ are listed in Table 1.

Thermogravimetric data for the title compound were collected on a Rigaku Thermoflex system. The sample was heated at a ramp rate of 20°C/min under flowing oxygen. Infrared data were collected from 4000 to 400 cm^{-1} using a Matteson FTIR spectrometer (KBr disk method).

0022-4596/98 $25.00

TABLE 1
Powder Data for $Ba_2(VO_2)(PO_4)(HPO_4)\cdot H_2O$

h	k	l	d_{obs} (Å)	d_{calc} (Å)	Δd	I_{rel}
0	0	1	10.767	10.800	−0.033	3
0	1	1	6.789	6.787	0.002	33
0	0	2	5.399	5.400	−0.001	27
1	0	0	5.066	5.066	0.001	13
0	2	0	4.366	4.362	0.004	13
0	2	1	4.046	4.045	0.001	26
1	0	2	3.669	3.669	−0.001	21
0	0	3	3.602	3.600	0.002	33
1	1	−2	3.422	3.422	0.000	96
1	1	2	3.381	3.382	−0.002	100
1	2	0	3.306	3.306	0.000	28
1	2	−1	3.166	3.169	−0.003	72
1	0	−3	2.957	2.954	0.003	13
1	0	3	2.917	2.915	0.001	9
1	2	−2	2.832	2.831	0.002	15
0	3	1	2.807	2.808	−0.001	54
0	1	4	2.580	2.579	0.001	51
0	3	3	2.262	2.262	0.000	29
0	4	1	2.138	2.138	0.000	23
1	2	−4	2.099	2.100	−0.002	36
1	3	3	2.058	2.059	−0.001	19
1	4	1	1.969	1.968	0.001	13
1	1	5	1.928	1.928	0.000	12
1	4	−2	1.881	1.882	0.000	16
2	3	−3	1.695	1.695	0.000	11
1	5	2	1.576	1.576	0.000	12

Single-crystal structure determination. A transparent plate (dimensions $\sim 0.1\times0.3\times0.4$ mm) of $Ba_2(VO_2)(PO_4)(HPO_4)\cdot H_2O$ was glued to a thin glass fiber with cyanoacrylate adhesive and mounted on a Siemens P4 automated diffractometer (graphite-monochromated Mo$K\alpha$ radiation, $\lambda = 0.71073$ Å). A primitive monoclinic unit cell was established and optimized by the application of peak-search, centering, indexing, and least-squares routines (54 peaks, $10 < 2\theta < 25^\circ$).

Intensity data were collected at room temperature [25(2)°C] using the $\theta/2\theta$ scan mode for $2 < 2\theta < 65^\circ$ ($-1\le h\le 7$, $-1\le k\le 13$, $-16\le l\le 16$). Intensity standards, remeasured every 100 observations, showed only statistical fluctuations over the course of the data collection. Absorption was monitored by ψ scans, and a correction (min 0.451, max 0.755) was applied at the data reduction stage. The raw intensities were reduced to F and $\sigma(F)$ values, the normal corrections for Lorentz and polarization effects were made, and the equivalent data were averaged: 2237 measured reflections merged to 2029 unique data [1893 considered observed according to the criterion $I > 3\sigma(I)$] with $R_{Int} = 2.84\%$.

The systematic absence condition in the reduced data ($0k0$, $k \neq 2n$) indicated space group $P2_1$ or $P2_1/m$, with intensity statistics suggesting the former. The main details of the $Ba_2(VO_2)(PO_4)(HPO_4)\cdot H_2O$ structure were established by Patterson methods (19) in space group $P2_1$ (No. 4). No reasonable starting atomic model could be established in space group $P2_1/m$, thus the noncentrosymmetric space group was assumed for the remainder of the refinement. The other non-hydrogen atoms were readily located from difference Fourier maps. Assuming the sole presence of vanadium(V) in this phase, the charge balancing requirement necessitates the presence of three protons per formula unit. We assume that one water molecule and one P–OH vertex account for the locations of these hydrogen atoms. These H atoms could not be located in difference Fourier syntheses; the hydrogen phosphate proton was placed geometrically (see below). Final residuals of $R = 2.65\%$ and $R_w = 2.89\%$ [$w_i = 1/\sigma^2(F)$] were obtained for refinements, varying a Larson-type extinction parameter (20), the Flack absolute structure parameter (21), and positional and anisotropic thermal parameters for all the atoms. The significant features in the final Fourier difference map were close to the Ba cations. The Flack parameter refined to $-0.05(2)$; thus the absolute structure of this phase is as shown in the Results section. Assuming the opposite absolute structure (Flack parameter fixed at 1.00) resulted in higher residuals of $R = 3.03\%$ and $R_w = 3.45\%$. All the least-squares refinements and subsidiary calculations were performed with the Oxford CRYSTALS (22) system. Crystallographic data are summarized in Table 2.

TABLE 2
Crystallographic Parameters for $Ba_2(VO_2)(PO_4)(HPO_4)\cdot H_2O$

Empirical formula	$Ba_2VP_2O_{11}H_3$
Formula weight	566.57
Crystal system	Monoclinic
a (Å)	5.0772(5)
b (Å)	8.724(2)
c (Å)	10.806(1)
β (deg)	90.795(8)
V (Å^3)	478.6(1)
Z	2
Space group	$P2_1$ (No. 4)
T (°C)	25(2)
λ (Mo$K\alpha$) (Å)	0.71073
ρ_{calc} (g/cm^3)	3.93
μ (cm^{-1})	94.5
Total no. of data	2237
No. of observed data[a]	1893
No. of Parameters	147
Min, max $\Delta\rho$ (e/Å^3)	−1.4, +2.0
$R(F)$[b] (%)	2.65
$R_w(F)$[c] (%)	2.89

[a] $I > 3\sigma(I)$ after data merging to 2029 unique reflections.
[b] $R = 100\times\sum||F_o| - |F_c||/\sum|F_o|$.
[c] $R_w = 100\times[\sum w(|F_o| - |F_c|)^2/\sum w|F_o|^2]^{1/2}$ with $w_i = 1/\sigma^2(F)$.

RESULTS

Crystal structure of $Ba_2(VO_2)(PO_4)(HPO_4)\cdot H_2O$. Atomic positional and thermal parameters are listed in Table 3, and selected geometrical data are presented in Table 4. This material adopts a new crystal structure built up from 11-coordinate barium cations, water molecules, and chains of vertex-sharing VO_5 trigonal bipyramids and tetrahedral PO_4/HPO_4 units, fused together via V–O–P bonds. The crystal structure of $Ba_2(VO_2)(PO_4)(HPO_4)\cdot H_2O$ is illustrated (23) in Fig. 1.

There are 16 unique non-hydrogen atoms in $Ba_2(VO_2)(PO_4)(HPO_4)\cdot H_2O$. The two barium cations both adopt irregular 11-fold coordination (Figs. 2 and 3), assuming a cutoff of 3.5 Å for the maximum Ba–O distance. Average Ba–O distances of 2.978(6) and 2.975(6) Å result for Ba(1) and Ba(2), respectively. Ba(1) includes two water molecules [atom O(11)] in its coordination sphere. Bond valence sums (BVS) calculated by the Brown formalism (24) of 2.04 for Ba(1) and 1.85 for Ba(2) (expected value = 2.00) show that Ba(1) satisfies its valence requirement, whereas Ba(2) is slightly "underbonded" in this structure.

The single vanadium species in $Ba_2(VO_2)(PO_4)(HPO_4)\cdot H_2O$ adopts a distinctive distorted trigonal bipyramidal coordination with respect to its five O atom neighbors (Fig. 4). Two short ($d < 1.65$ Å) bonds to O(1) and O(2) form two of the three equatorial vertices of this polyhedron [$\theta\{O(1)–V–O(2)\} = 106.3(3)^\circ$]. The three remaining vertices form parts of V–O–P links, with a resulting O–V–O bond angle of 160.8(2)° for the two axial links. The bond valence sum for V is 4.96 (expected value for vanadium(V) character = 5.00). The VO_5 polyhedron is somewhat distorted. Axial–equatorial O···O contacts cover a fairly narrow range from 2.55 to 2.76 Å (average = 2.66 Å); however, the equatorial O···O contact between O(1) and O(2) (2.61 Å) is much shorter than the O(1)···O(3) and O(2)···O(3) nonbonding contacts (3.17 and 3.31 Å, respectively). Within the O_5 polyhedron (volume = 5.09 Å^3), the V atom has made a nominal shift of 0.143 Å from the centroid (25) of this group towards an equatorial edge, resulting in the two short V=O links noted above. The equatorial V(1), O(1), O(2), O(5) grouping is planar to within 0.06 Å.

The phosphorus atoms show typical tetrahedral coordination [d_{av}(P(1)–O) = 1.539(5) Å, BVS[P(1)] = 4.96; d_{av}(P(2)–O) = 1.539(5) Å, BVS[P(2)] = 4.95]. The P(1) centered group makes one P–O–V link and has three terminal P–O bonds, one of which is assumed to be protonated, as P(1)–O(6)H, on the basis of its length (26). The $P(2)O_4$ group makes two P–O–V links, and has two terminal P–O bonds. There is one water molecule of crystallization [oxygen atom O(11)].

TABLE 3
Atomic Coordinates/Thermal Factors for $Ba_2(VO_2)(PO_4)(HPO_4)\cdot H_2O$

Atom	x	y	z	U_{eq}[a]
Ba(1)	0.03246(8)	0.49849(9)	0.04342(4)	0.0142
Ba(2)	0.00970(7)	0.84018(9)	0.38855(4)	0.0124
V(1)	0.4416(2)	0.4996(2)	0.3294(1)	0.0098
P(1)	0.4870(3)	0.7772(2)	0.1456(2)	0.0104
P(2)	0.4635(3)	0.1491(2)	0.4205(2)	0.0094
O(1)	0.558(1)	0.4136(7)	0.2080(5)	0.0202
O(2)	0.1320(9)	0.5350(7)	0.2985(5)	0.0159
O(3)	0.548(1)	0.7128(6)	0.2777(5)	0.0148
O(4)	0.376(1)	0.3176(6)	0.4346(5)	0.0159
O(5)	0.673(1)	0.5612(7)	0.4716(5)	0.0135
O(6)	0.628(1)	0.9386(7)	0.1472(5)	0.0190
O(7)	0.607(1)	0.6840(9)	0.0454(5)	0.0264
O(8)	0.1908(9)	0.8025(7)	0.1310(5)	0.0173
O(9)	0.353(1)	0.0817(7)	0.2997(5)	0.0183
O(10)	0.760(1)	0.1339(7)	0.4332(6)	0.0221
O(11)	0.981(1)	0.2117(7)	0.1559(5)	0.0193

[a] U_{eq} (Å^2) = $\frac{1}{3}[U_1 + U_2 + U_3]$.

TABLE 4
Selected Bond Distances (Å) and Angles (°) for $Ba_2(VO_2)(PO_4)(HPO_4)\cdot H_2O$

Ba(1)–O(1)	3.105(5)	Ba(1)–O(1)	3.271(6)
Ba(1)–O(2)	2.813(5)	Ba(1)–O(6)	2.755(5)
Ba(1)–O(7)	2.699(6)	Ba(1)–O(7)	3.336(7)
Ba(1)–O(7)	3.442(8)	Ba(1)–O(8)	2.925(6)
Ba(1)–O(8)	2.775(5)	Ba(1)–O(11)	2.795(6)
Ba(1)–O(11)	2.846(6)	Ba(2)–O(2)	2.905(6)
Ba(2)–O(3)	2.845(5)	Ba(2)–O(3)	3.198(6)
Ba(2)–O(4)	2.763(5)	Ba(2)–O(5)	3.113(6)
Ba(2)–O(5)	2.920(5)	Ba(2)–O(6)	3.340(6)
Ba(2)–O(8)	2.961(5)	Ba(2)–O(9)	2.906(6)
Ba(2)–O(10)	2.902(6)	Ba(2)–O(10)	2.873(6)
V(1)–O(1)	1.629(6)	V(1)–O(2)	1.632(5)
V(1)–O(3)	2.017(6)	V(1)–O(4)	1.983(6)
V(1)–O(5)	1.996(5)	P(1)–O(3)	1.560(5)
P(1)–O(6)	1.579(6)	P(1)–O(7)	1.492(6)
P(1)–O(8)	1.526(5)	P(2)–O(4)	1.544(6)
P(2)–O(5)	1.566(6)	P(2)–O(9)	1.530(6)
P(2)–O(10)	1.516(5)		
O(1)–V(1)–O(2)	106.3(3)	O(1)–V(1)–O(3)	95.8(3)
O(2)–V(1)–O(3)	91.7(3)	O(1)–V(1)–O(4)	99.1(3)
O(2)–V(1)–O(4)	95.7(3)	O(3)–V(1)–O(4)	160.8(2)
O(1)–V(1)–O(5)	121.9(3)	O(2)–V(1)–O(5)	131.5(3)
O(3)–V(1)–O(5)	78.9(2)	O(4)–V(1)–O(5)	82.9(2)
O(3)–P(1)–O(6)	103.2(3)	O(3)–P(1)–O(7)	113.0(4)
O(6)–P(1)–O(7)	107.7(4)	O(3)–P(1)–O(8)	109.2(3)
O(6)–P(1)–O(8)	108.5(3)	O(7)–P(1)–O(8)	114.6(3)
O(4)–P(2)–O(5)	105.2(3)	O(4)–P(2)–O(9)	110.3(3)
O(5)–P(2)–O(9)	106.6(3)	O(4)–P(2)–O(10)	111.1(3)
O(5)–P(2)–O(10)	109.9(3)	O(9)–P(2)–O(10)	113.3(3)
V(1)–O(3)–P(1)	122.3(3)	V(1)–O(4)–P(2)	130.9(3)
V(1)–O(5)–P(2)	116.3(3)		

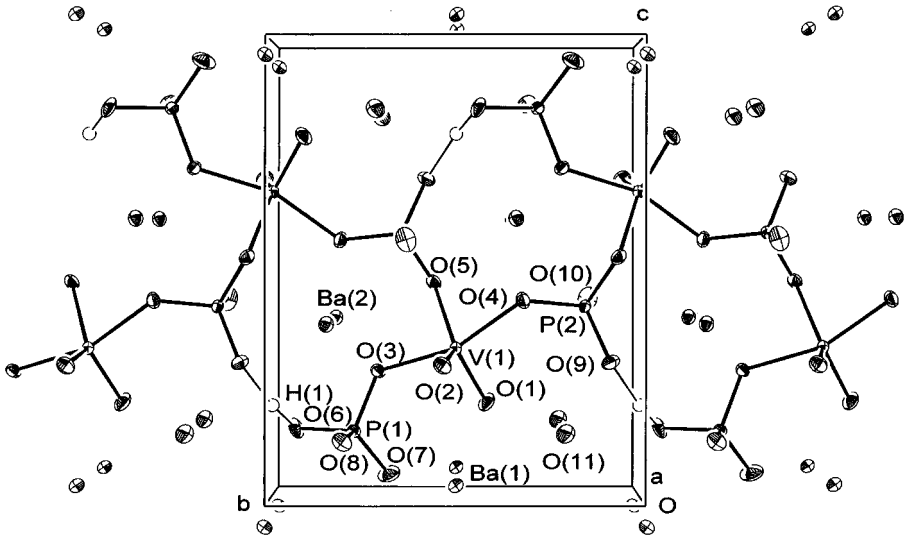

FIG. 1. View down [100] of the crystal structure of $Ba_2(VO_2)(PO_4)(HPO_4)\cdot H_2O$ showing the infinite $[(VO_2)(PO_4)(HPO_4)]^{4-}$ chain. The proposed intrachain H bonding linkage is indicated as a thin line. Ba–O bonds are omitted for clarity (50% thermal ellipsoids; arbitrary sphere for H atom).

Of the 11 O atoms in the structure, O(1) and O(2) are terminal to V and may be regarded as parts of V=O "vanadyl" double bonds. Their individual bond valences are more than double those of the longer V–O bonds. Atoms O(3), O(4), and O(5) form V–O–P bridges ($\theta_{av} = 123.2^\circ$), and O(6)–O(10) are terminal P–O vertices, all of which also form part of one or more Ba–O contacts. The water molecule oxygen atom, O(11), bonds to two Ba(1) cations and has contacts to O(9) [$d(O\cdots O) = 2.681(8)$ Å], O(1) [2.840(8) Å], O(6) [2.985(9) Å], and O(7) [3.048(7) Å] which might represent H bonding links.

The polyhedral connectivity in $Ba_2(VO_2)(PO_4)(HPO_4)\cdot H_2O$ results in contorted, infinite chains of VO_5 and P(2)O_4 groups propagating along the polar [010] direction (Fig. 1). The P(1)O_4 group also bonds to the vanadium center, but it does not partake in the chain connectivity. Based on geometrical placement of the H atom, a strong intrachain hydrogen bond exists between two phosphate groups (Fig. 1), as an O(6)–H(1)$\cdots$O(9) link [$d(H\cdots O) = 1.50$ Å]. However, when P–O and Ba-O interactions are taken into account, the bond valence sums of O(6) and O(9) are both ~ 1.46. Thus, the possibility of a symmetrical O(6)$\cdots$H$\cdots$O(9) or disordered [both O(6)–H(1)$\cdots$O(9) and O(6)$\cdots$H(1)–O(9) conformations present] hydrogen bond cannot be ruled out. Interchain connectivity is through barium cations and possibly via H-bonding interactions

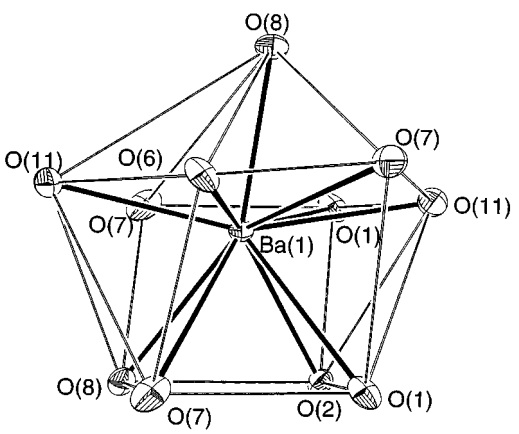

FIG. 2. Detail of the Ba(1) coordination environment in $Ba_2(VO_2)(PO_4)(HPO_4)\cdot H_2O$ with nonbonding O$\cdots$O contacts < 4.0 Å indicated by thin lines.

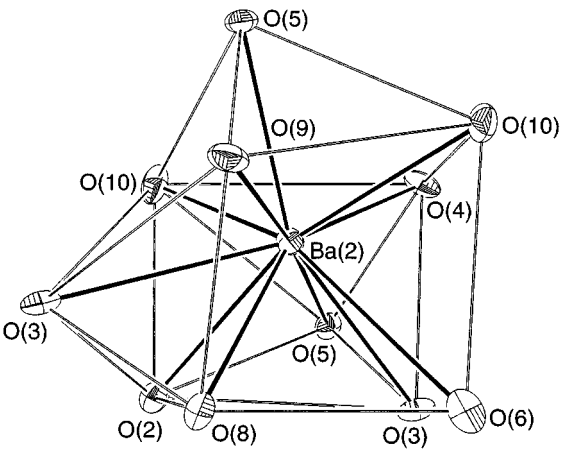

FIG. 3. Detail of the Ba(2) coordination environment in $Ba_2(VO_2)(PO_4)(HPO_4)\cdot H_2O$ with nonbonding O$\cdots$O contacts < 4.0 Å indicated by thin lines.

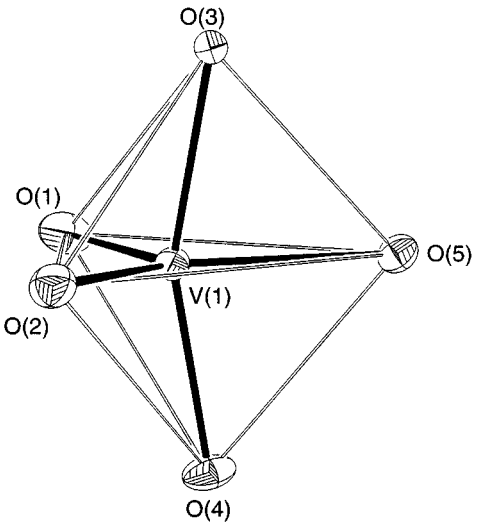

FIG. 4. Detail of the VO_5 trigonal bipyramidal grouping in $Ba_2(VO_2)(PO_4)(HPO_4)\cdot H_2O$.

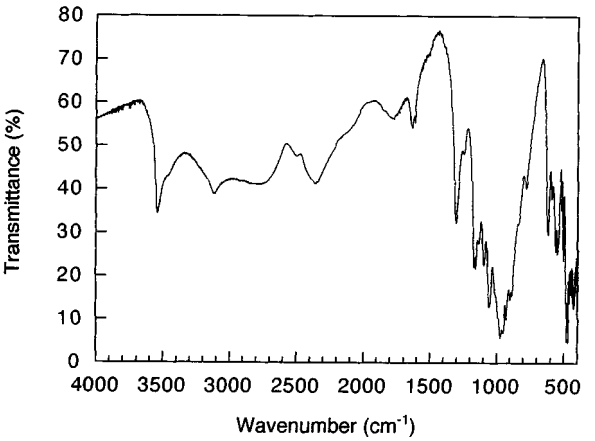

FIG. 5. IR spectrum of $Ba_2(VO_2)(PO_4)(HPO_4)\cdot H_2O$.

involving the O(11) water molecule. Considered separately, the Ba/O network includes triangular face-sharing and edge-sharing connectivity between the BaO_{11} polyhedra.

Physical Data

TGA for $Ba_2(VO_2)(PO_4)(HPO_4)\cdot H_2O$ showed two endothermic weight loss events (-3% over the temperature range $\sim$330–390°C, and -1.2% at $\sim$500–560°C). The first of these probably corresponds to loss of the extrachain water molecule (calc. -3.2%), and the second may arise from breakdown of the HPO_4 group to yield $\frac{1}{2}H_2O$ (calc. -1.6%), leaving a nominal residue of $Ba_2VP_2O_{9.5}$. A third endotherm at $\sim$680°C was not accompanied by an observable weight change and may arise from a phase transformation or melting/decomposition.

The infrared spectrum of $Ba_2(VO_2)(PO_4)(HPO_4)\cdot H_2O$ (Fig. 5) shows bands due to PO_4 and water modes in the region 2800–3200 and 3500 cm^{-1}. The complex group of bands in the 800–1300 cm^{-1} region arises from partially resolved PO_4 and VO modes.

DISCUSSION

We have prepared and characterized another BaVPO phase, complementing the materials listed in Table 5. As is typical of the seemingly limitless structural diversity of vanadium phosphates, $Ba_2(VO_2)(PO_4)(HPO_4)\cdot H_2O$ shows no particular similarities to any of the previously characterized BaVPOs. A large excess of phosphoric acid was required to synthesize $Ba_2(VO_2)(PO_4)(HPO_4)\cdot H_2O$ in measurable yield, which perhaps signifies that the acid is playing a dual role in supplying phosphate ions and controlling pH in the hydrothermal reaction.

The trigonal bipyramidal geometry of the VO_5 group in $Ba_2(VO_2)(PO_4)(HPO_4)\cdot H_2O$ is distinctive and unusual in vanadium solid state chemistry and has not been previously seen in BaVPOs. A similar local VO_5 geometry arises in $KVO_3\cdot H_2O$ (27) as part of a "double-chain" metavanadate $[(VO_3)_n]$ ion. In this phase, there are two terminal V=O bonds and three V–O–V′ links in the infinite double chains. One way of viewing the metavanadate double chain is in terms of the nominal fusing together of parallel chains of distorted tetrahedra (28). V_2O_5 contains a different, highly distorted VO_5 grouping, which is closer to square pyramidal (29). The more common square pyramidal VO_5 geometry

TABLE 5
Summary of Barium Vanadium Phosphate Phases[a]

Phase	Ratio	Ox.	Coord.	Dim.	Ref.
$Ba(VO_2)(PO_4)$	1:1:1	V	D	2D	4
$Ba(VO)(PO_4)(H_2PO_4)\cdot H_2O$	1:1:2	IV	D	2D	9
$Ba(VO)_2(PO_4)_2$	1:2:2	IV	D + S	2D	1
$Ba(VOPO4)_2\cdot 4H_2O$	1:2:2	IV	S	2D	11
α-$BaV_2(P_2O_7)_2$	1:2:4	III	O	3D	2
β-$BaV_2(P_2O_7)_2$	1:2:4	III	O	3D	6
$BaV_2(HPO_4)_4\cdot H_2O$	1:2:4	III	O	3D	5
$Ba_2(VO)(PO_4)_2\cdot H_2O$	2:1:2	IV	D	1D	7
$Ba_2(VO_2)(PO_4)(HPO_4)\cdot H_2O$	2:1:2	V	B	1D	This work
$Ba_2(VO)(PO_4)_2$	2:1:2	IV	D	2D	10
$Ba_2V_3H(PO_4)_2(P_2O_7)_2$	2:3:6	III	O	3D	3
$Ba_2V_5O_8(PO_4)_4$	2:5:4	IV+V	T+S+D	3D	13
$Ba_3V_2O_3(PO_4)_3$	3:2:3	IV+V	S+D	1D	14
$Ba_3V_4(PO_4)_6$	3:4:6	III	O	3D	12[b]
$Ba_8(VO)_6(PO_4)_2(HPO_4)_{11}\cdot 3H_2O$	8:6:13	IV	D	1D	8

[a] **Ratio**, Ba:V:P ratio; **Ox**, V oxidation state; **Coord**, vanadium coordination polyhedron type (O = octahedral, D = distorted octahedral, S = square pyramidal, B = trigonal bipyramidal, T = tetrahedral); **Dim**, dimensionality of V/P/O network (3D = continuous network, 2D = layers, 1D = chains).

[b] Langbeinite structure type identified from powder diffraction data.

(short, apical V=O bond and four longer equatorial V–O links) occurs in many inorganic phases such as $K(VO_2)(HPO_4)$ (30), which consists of one-dimensional chains of VO_5 and PO_4 groups, linked via V–O–V and V–O–P bonds.

Referring to Table 5, we see that vanadium(III)-containing BaVPOs are inevitably three-dimensional in their polyhedral connectivity throughout the structure, whereas the vanadium(IV) and vanadium(V) BaVPOs tend toward lower dimensionality (layers and chains). Even for a particular Ba : V : P compositional ratio, there is striking structural diversity, which is due in part to versatility of the phosphate group (its ability to form P–O–V, P–O, or P–OH links), and the lack of a strong coordination preference for the Ba^{2+} cation. However, the packing requirements of the bulky Ba^{2+} species in barium-rich phases (14) may also promote the formation of lower-dimensional VPO structures.

ACKNOWLEDGMENT

We thank the Australian Research Council for financial support.

REFERENCES

1. A. Grandin, J. Chardon, M. M. Borel, A. Leclaire, and B. Raveau, *J. Solid State Chem.* **99,** 297 (1992).
2. L. Benhamada, A. Grandin, M. M. Borel, A. Leclaire, and B. Raveau, *Acta Crystallogr., Sect. C* **47,** 2437 (1991).
3. E. Dvoncova, K.-H. Lii, C.-H. Li, and T.-M. Chen, *J. Solid State Chem.* **106,** 485 (1993).
4. H.-Y. Kang, S.-L. Wang, and K.-H. Lii, *Acta Crystallogr., Sect. C* **48,** 975 (1992).
5. Z.-W. Wang, R. C. Haushalter, M. E. Thompson, and J. Zubieta, *Mater. Chem. Phys.* **35,** 205 (1993).
6. S.-J. Hwu, R. I. Carroll, and D. L. Serra, *J. Solid State Chem.* **110,** 290 (1994).
7. W. T. A. Harrison, S. C. Lim, J. T. Vaughey, A. J. Jacobson, D. P. Goshorn, and J. W. Johnson, *J. Solid State Chem.* **113,** 444 (1994).
8. W. T. A. Harrison, J. T. Vaughey, A. J. Jacobson, D. P. Goshorn, and J. W. Johnson, *J. Solid State Chem.* **116,** 77 (1995).
9. W. T. A. Harrison, S. C. Lim, L. L. Dussack, A. J. Jacobson, D. P. Goshorn, and J. W. Johnson, *J. Solid State Chem.* **118,** 241 (1995).
10. C. Wadewitz and H. Müller-Buschbaum, *Z. Naturforschung.* **B51,** 1290 (1996).
11. M. Roca, M. D. Marcos, P. Amorós, J. Alamo, A. Beltrán-Porter, and D. Beltrán-Porter, *Inorg. Chem.* **36,** 3414 (1997).
12. K. Kasthuri Rangan and J. Gopalakrishnan, *J. Solid State Chem.* **109,** 116 (1994).
13. M. M. Borel, A. Leclaire, J. Chardon, and B. Raveau, *J. Mater. Chem.* **8,** 693 (1998).
14. M. M. Borel, A. Leclaire, J. Chardon, C. Michel, J. Provost, and B. Raveau, *J. Solid State Chem.* **135,** 302 (1998).
15. G. Burley, *J. Res. Natl. Bur. Stds., Sect. A.* **60,** 23 (1958).
16. F. C. Hawthorne and C. Calvo, *J. Solid State Chem.* **22,** 157 (1977).
17. K. Yvon, K, W. Jeitschko, and E. Parthe, *J. Appl. Crystallogr.* **10,** 73 (1977).
18. J. Lauglier and A. Filhol, "Program ERACEL." Version distributed by A. Le Bail, University of Le Mans, France, 1997.
19. G. M. Sheldrick, "SHELXS86 User Guide." University of Göttingen, Germany, 1986.
20. A. C. Larson, *Acta Crystallogr.* **23,** 664 (1967).
21. H. D. Flack, *Acta Crystallogr., Sect. A* **39,** 876 (1983).
22. D. J. Watkin, J. R. Carruthers, and P. W. Betteridge, "CRYSTALS User Guide." Chemical Crystallography Laboratory, Oxford University, UK, 1996.
23. L. Farrugia, "ORTEP32 (Windows 95 version) User Guide." University of Glasgow, UK, 1997.
24. I. D. Brown, *J. Appl. Crystallogr.* **29,** 479 (1996).
25. T. B. Zunic and I. Vickovic, *J. Appl. Crystallogr.* **29,** 305 (1996).
26. P. Lightfoot and D. Masson, *Acta Crystallogr., Sect. C* **52,** 1077 (1996).
27. C. L. Christ, J. R. Clark, and H. T. Evans, *Acta Crystallogr.* **7,** 801 (1954).
28. A. F. Wells, "Structural Inorganic Chemistry," 5th ed., p. 567. Oxford Univ. Press.
29. H. G. Bachmann, F. R. Ahmed, and W. H. Barnes, *Zeit. Kristallogr.* **115,** 110 (1961).
30. P. Amoros, D. Beltran-Porter, A. Le Bail, G. Férey, and G. Villeneuve, *Eur. J. Solid State Inorg. Chem.* **25,** 599 (1988).